Integrated Ferroelectrics ›
An International Journal
Volume 205, 2020 - Issue 1: Proceedings of the International Conference on Nano-Structured Materials and Devices (ICNSMD-2018): Part IV of IV

E: Nanostructured Materials (continued)

Synthesis and Luminescence Properties of Eu^{3+} Doped Sr_2SiO_4 Phosphor

D. S. Bobade & P. B. Undre

Pages 72-80 | Received 01 Oct 2018, Accepted 12 Aug 2019, Published online: 09 Feb 2020

Cite this article https://doi.org/10.1080/10584587.2019.1675001 Check for updates

Abstract

The europium doped Sr_2SiO_4 phosphors were prepared by the combustion synthesis technique. The prepared samples of europium doped Sr_2SiO_4 phosphors were characterized by X-Ray Diffraction (XRD), Ultraviolet Visible spectroscopy (UV), Fourier Transform Infrared Spectroscopy (FT-IR), Field Emission Scanning Electron Microscopy (FE-SEM), Energy Dispersive Spectra (EDS) and Photoluminescence Technique (PL). The orthorhombic crystal structure of the prepared sample was confirmed by using XRD. The formation of fiber like nano structured nature was confirmed by the images captured using the FE-SEM technique. The band gap energies were calculated using the UV-Visible spectra of the samples and these band gap energies were observed as 4.5826 eV for Sr_2SiO_4 and 4.1748 eV for Eu (5 m%) doped Sr_2SiO_4.

One peak was observed at the 590 nm under 393 nm excitation and another peak was observed at the 615 nm under 408 nm excitation. The CIE color coordinates of the Eu^{3+} doped Sr_2SiO_4 phosphors are $x \approx 0.6615$, $y \approx 0.3382$ (red color) observed for 408 nm excitation and $x \approx 0.5636$, $y \approx 0.4356$ (orange) observed for 393 nm excitation calculated using the color calculator program radiant imaging.

Keywords: Phosphor combustion synthesis PL EDS FT-IR XRD FE-SEM

1. Introduction

The rare earth element activated phosphor materials have been investigated in recent 30 years and are applied in different fields. These rare earth elements attracted the minds of people because of their characteristic emission in visible and near visible (ultraviolet) regions. These emissions in visible region are attributed to the 5d → 4f transitions. Among these, the europium ion activated phosphors have been attracted much interest of researchers due to the characteristic emission of europium ions in the visible region. The europium ion activated phosphors has been applied in many field like display devices, solid state lighting, radiation dosimetry, x-ray imaging, CRO tubes [1–4], LED's and Hg discharge lamps [5–8]. It is known that the luminescence property of the europium ion is strongly influenced by the surrounding crystal field and the symmetry acquired by it [9–11]. Basically silicate materials have appropriate properties as far as application point view due to their excellent temperature stability, water resistance and capable to show the luminescence property when doped with the rare earth element and transition element.

The europium in the host lattice acquires the two types of the states as Eu^{2+} and Eu^{3+} depending upon the crystal structure of host material. The Eu^{2+}state acquired by the europium is depending on crystal field strength created due to surrounding legands. The emission due to Eu^{2+} state affected by the size, charge and strength of the ligand to metal ion bonding due to the surrounding legands [12, 13]. This emission is well known as 5f → 4d ($^4f_6{}^5d_1 \rightarrow {}^4f_7$) transition which is broad band emissioncovers the large wavelength region from ultraviolet to yellow.

The Eu^{3+} state is created due to oxidation of Eu^{2+} from the local symmetry acquired by the

In this article

emission of Eu^{3+} is made up of narrow lines occurring at longer wavelengths (red or orange luminescence) of the visible region and these emissions are mainly with the transition from lowest excited state $^5D_0$ to discrete ground states ^7F_j within $^4f_6$ configuration [13, 14].

Recently different silicates phosphors activated with europium ion were prepared, studied and investigated [15–19]. From this, it is observed that the europium doped silicates phosphor having potential applications in different fields of lighting.

The detailed analysis of the prepared Eu^{3+} doped Sr_2SiO_4 phosphors using solution combustion synthesis is done by UV-Visible spectroscopy, FT-IR spectroscopy, X-ray powder diffraction, FE-SEM technique, EDS-spectroscopy and photoluminescence technique.

2. Experimental

2.1. Phosphor Preparation

Many researchers have been used the combustion synthesis technique which is easy and less assembly required method for the preparation the samples. The Eu^{3+} doped Sr_2SiO_4 nano phosphors were prepared by using the combustion synthesis technique using 99.9% AR grade (Loba Chemie) high purity samples $Sr(NO_3)_2$ 6 H_2O, SiO_2 x H_2O, $(NH_4)(NO_3)$, and Eu_2O_3 and Nitric Acid as raw materials and urea was used as fuel agent for the combustion process. Eu_2O_3 was first weighed with stoichiometric ratio and dissolved in 3 ml nitric acid with warm heating. Other precursors with stoichiometric ratio were dissolved in the 20 ml distilled water and also dissolved Eu_2O_3 in nitric acid is mixed in the prepared solution and this solution was stirred for 30 min. After stirring the homogenous solution was obtained and this solution was placed in the muffle furnace which was maintained 500 °C. The placed solution was boiled and ignition took place due to the urea. During ignition gases are evolved and foamy material was formed with evolution of gases. Here urea was used as fuel agent and during ignition the temperature became to near 1500 °C, this results into the formation nano powdered samples. The molar concentration of Eu_2O_3 was varied as 1 m%, 2 m%, 5 m% and 10 m% to replace the Sr^{2+} from the host Sr_2SiO_4 host. The prepared powder samples were characterized by the UV spectroscopy, FT-IR Spectroscopy, FE-SEM Technique, XRD technique and PL measurement.

In this article

3. Results and Discussion

3.1. UV-Visible Spectroscopy Analysis

UV-V Spectroscopy technique is important technique to study the energy band gap of the materials. The Figure 1a represents UV absorbance of the prepared samples Sr_2SiO_4 host and Figure 1b represents Sr_2SiO_4:Eu. The energy band gaps are calculated using the absorption edge and these energy band gaps for host Sr_2SiO_4 and Eu^{3+} doped Sr_2SiO_4 are found to be 4.5926 eV and 4.1748 eV respectively. From this, it is observed that the band gap of host Sr_2SiO_4 decreases to 4.1748 eV for 5 m% doping of Eu^{3+}. The small red shift was occurred in absorption for 5 m% Eu^{3+} doped Sr_2SiO_4 to energy levels acquired by the Eu^{3+} ion in the energy band gap. The change in intensity is observed for Eu^{3+}doping due to the energy levels acquired by the europium in energy band gap of the host. Therefore, more number of electrons acquired excited states due to absorption of the incident photon energy. From this discussion it cleared that the energy band can be modulated by doping of Eu^{3+} ions, since acquiring the interstitial positions of energy levels in the host energy gap. Therefore, the Eu^{3+} is used to acquire the certain properties like the photoluminescence.

Figure 1. UV-visible absorbance spectra of (a) Sr_2SiO_4 host and (b) Sr_2SiO_4: Eu (5 m%).

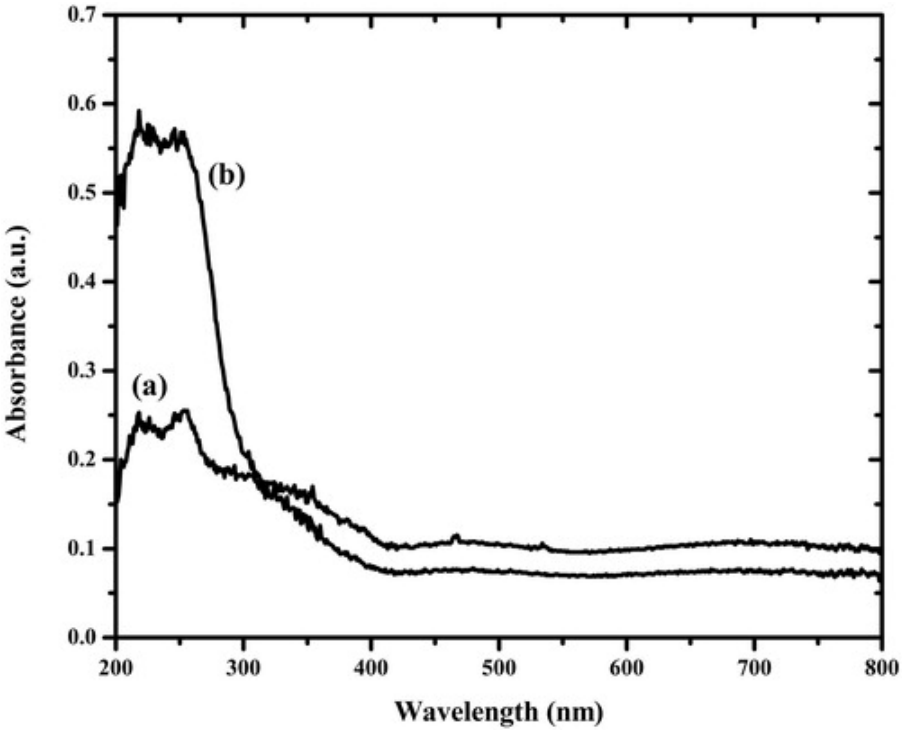

Display full size

In this article

3.2. FT-IR Spectroscopy Analysis

Figure 2a depicts the FT-IR Spectra of the Sr_2SiO_4 host and Figure 2b denotes Sr_2SiO_4:Eu (5 m%) samples. The strong absorption band is observed at 1480 cm^{-1} which is ascribed to Sr-O stretching vibration and also most of the incident energy was utilized for the stretching vibrations of Sr-O bond [20, 21]. The absorption in the range of 500–557 cm^{-1} is due to stretching vibrations and bending vibration Si-O bond [21, 22]. The absorption band in the 800–1000 cm^{-1} region is resulted due to the stretching vibrations of Si-O-Si linkages in the SiO_4 tetrahedron unit [20–21]. The absorption peaks after 3500 cm^{-1} are due to H-O-H bond vibrations of absorbed water [20–22]. From FT-IR analysis, it is cleared that the bonding nature of the sample is consistent to the noted results by the researchers.

Figure 2. FT-IR Spectra of (a) Sr_2SiO_4 host and (b) Sr_2SiO_4: Eu (5 m%).

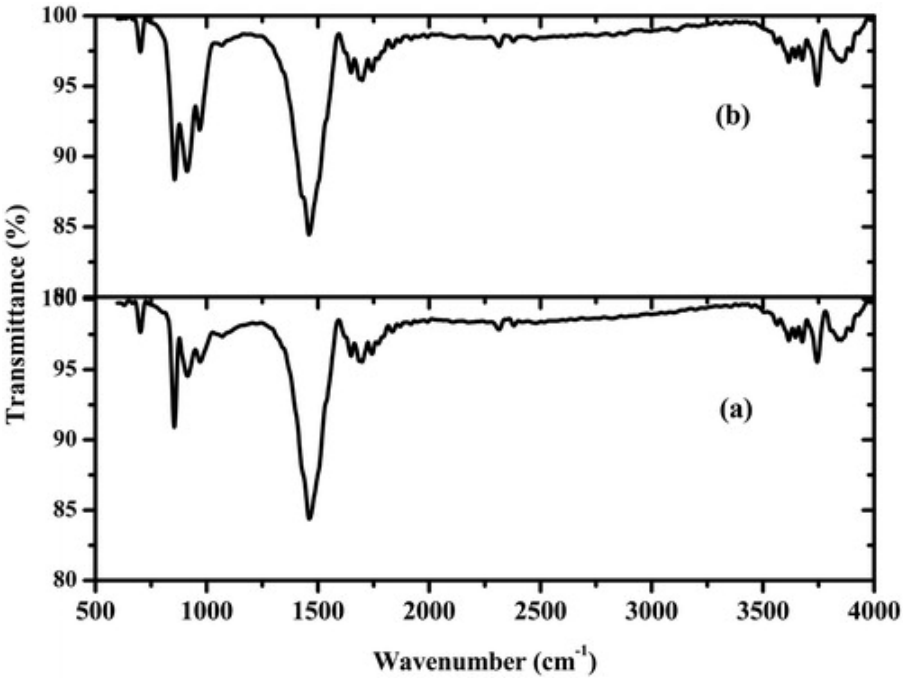

Display full size

3.3. X-Ray Diffraction Studies

The XRD technique is very important technique to study the structural study of the materials. Figure 3 denotes the XRD powder diffraction patterns of the host Sr_2SiO_4 and Sr_2SiO_4: Eu (5 m%) and were well match with the ICCD database number 76-1494. It has shown orthorhombic structure with cell parameters a = 2.83, b = 2.87 and c = 2.84 with space group Pnma (65) [23,

In this article

crystalline nature of the prepared host Sr_2SiO_4 sample.

Figure 3. X-Ray diffraction pattern of Sr_2SiO_4 host and Sr_2SiO_4: Eu (5 m%).

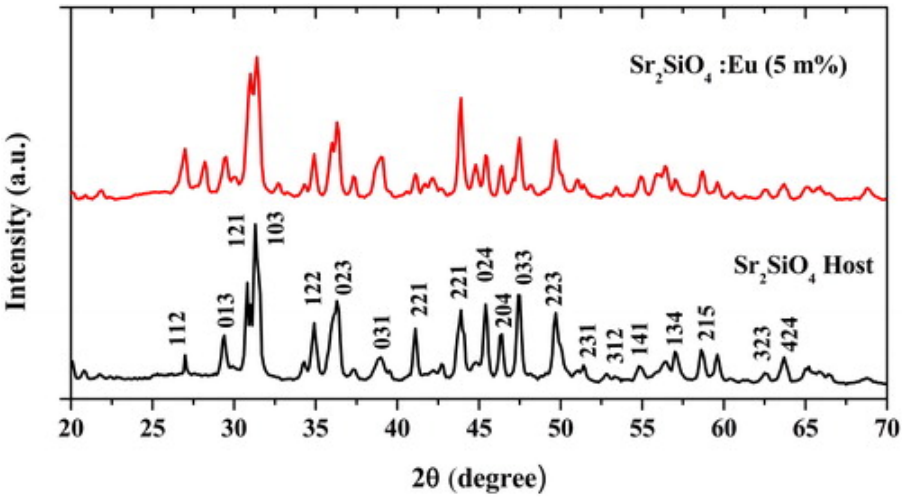

Display full size

An average crystalline size for the sample is estimated from full width at half maximum of diffraction pattern using Scherer's formula,

$$D = \frac{0.94\,\lambda}{\beta \cos \theta}$$

(1) Where, D is the crystalline size, λ is the wavelength (for Cu Kα, λ = 1.5406 A^0), β is the full width at half maximum (FWHM) and θ is the Bragg's angle. The estimated an average particle size is 90 nm.

3.4. FE-SEM Analysis

We have studied the morphological study of the prepared samples using FE-SEM technique. Figure 4 depicts the FE-SEM images of the prepared Sr_2SiO_4 host material. From the FE-SEM images, it is observed that the prepared Sr_2SiO_4 host material having nano fiber shaped particles and these are also agglomerated to some extent. An average crystalline width of these particles is found to be 44 nm.

Figure 4. FE-SEM images of Sr_2SiO_4: Eu (5 m%).

In this article

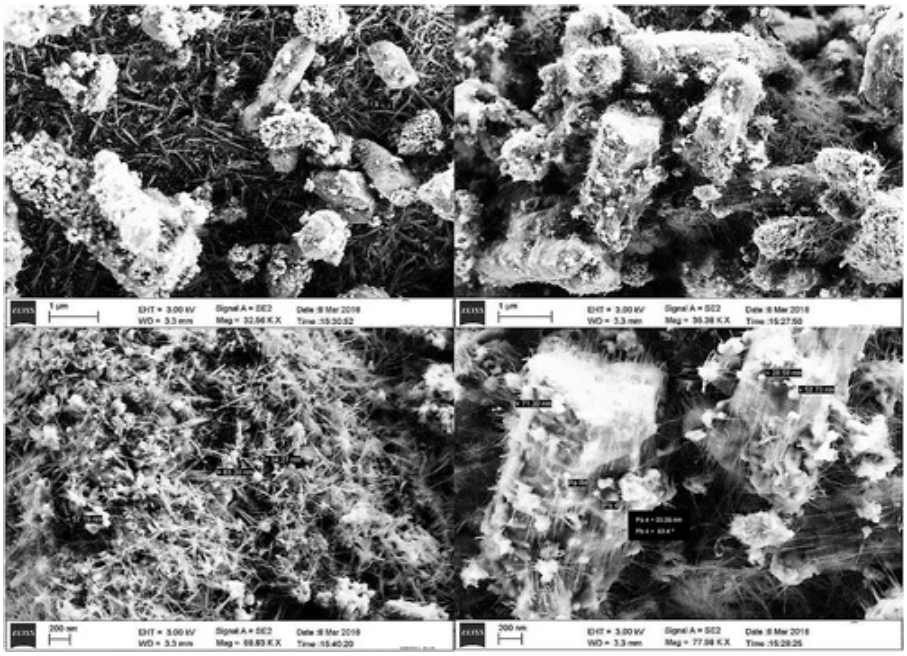

Display full size

3.5. EDS Studies

Figure 5 shows the EDS spectrum and elemental composition analysis of the Sr_2SiO_4:Eu (5 m%). The EDS spectrum of Sr_2SiO_4:Eu shows the count pecks with certain energy for Sr, Si, O and Eu in prepared Sr_2SiO_4:Eu material. The elemental composition is shown in table format in the Figure 5. The atomic and weight % is well seen in the prepared Sr_2SiO_4:Eu. It confirmed the formation of the required compositions of the sample.

Figure 5. EDS Spectra and atomic % of Sr_2SiO_4:Eu (5 m%).

In this article

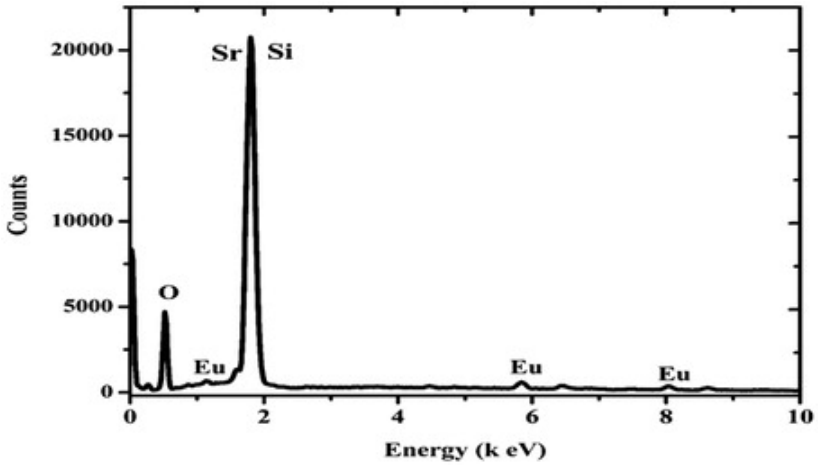

Elements	Weight%	Atomic%
O K	45.93	77.30
Si K	10.02	9.60
Sr L	40.64	12.50
Eu L	3.41	0.60
Total	100	100

Display full size

3.6. PL Measurements

The prepared Eu^{3+} doped Sr_2SiO_4 phosphor characterized by the photoluminescence technique. Figure 6a represents the excitation spectra of the 1 and 5 m% europium doped Sr_2SiO_4 phosphor monitored under 590 nm emission. In emission spectra, the strong absorption is observed at the 393 nm wavelength due to the $^7F_0 \rightarrow {}^5F_1$ transition of europium ions in the host Sr_2SiO_4.

Figure 6. (a) Excitation spectra of Sr_2SiO_4:Eu monitored under 590 nm emission and (b) emission spectra of Sr_2SiO_4:Eu monitored under 393 nm excitation.

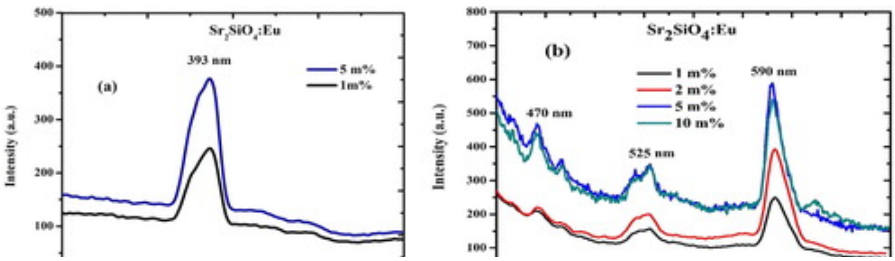

In this article

Display full size

Figure 6b represents the emission spectra of the Eu^{3+} doped Sr_2SiO_4 phosphor monitored under 393 nm excitation wavelength. This showed the prominent peck is at 590 nm (orange) which is due to the $^5D_0 \rightarrow {}^7F_1$ transitions of the Eu^{3+} ion. This transition is noted due to the Eu^{3+} ion acquired the low site symmetry site and also this transition is regardless of the surrounding atmosphere. This transition is also known as magnetic dipole transition [25–27].This turn the Sr_2SiO_4 phosphor is may be suitable to be used for near UV excitation orange phosphor for solid state lighting.

It is also seen that the 1 m% and 5 m% Eu^{3+} doped Sr_2SiO_4 phosphors when monitored under 615 nm emission, they have shown the excitation peck centered at 408 nm as shown in Figure 7a. This transition in excitation spectra is corresponding to $^7F_0 \rightarrow {}^5D_3$ in europium ion. Figure 7b denotes the emission spectra of the Eu^{3+} doped Sr_2SiO_4 phosphors monitored under the 408 nm excitation. This transition is assigned to the electric dipole transition carried out in the Eu^{3+} ion from $^5D_0 \rightarrow {}^7F_1$ and this transition varies with the surrounding crystal field strength [13]. The Sr_2SiO_4 doped with the europium ion, the Eu^{3+} has occupied the two characteristic different sites of Sr (I) and Sr (II) resulted in the creation of luminescence property.

Figure 7. (a) Excitation spectra of Sr_2SiO_4:Eu monitored under 615 nm emission and (b) emission spectra of Sr_2SiO_4:Eu monitored under 408 nm excitation.

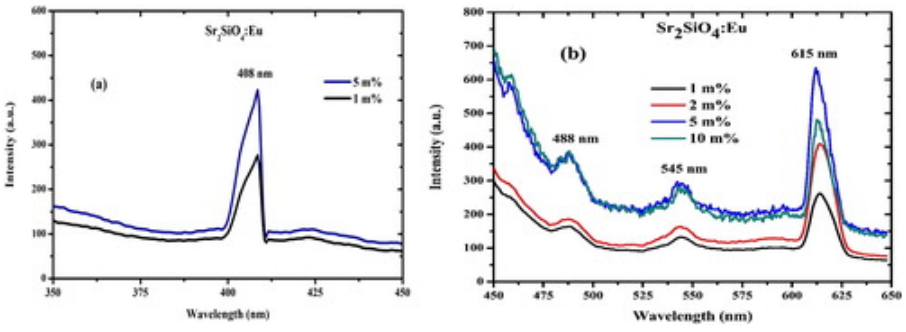

Display full size

3.7. Color Co-Ordinates

The chromatic coordinates (x, y) was calculated using the color calculator program radiant imaging refer to the 1931 CIE Standard Source C (illuminant Cs (0.3101, 0.3162)) [28]. The

In this article

emission at 590 nm and red color ($x \approx 0.\ 0.6644$, $y \approx 0.\ 3216$) for emission at 615 nm are shown in Figure 8 by points A and B (white circles) respectively. This indicates that the color properties of the phosphor powder prepared by combustion synthesis do approaching requirements of solid state lighting.

Figure 8. Color co-ordinates of Sr_2SiO_4:Eu.

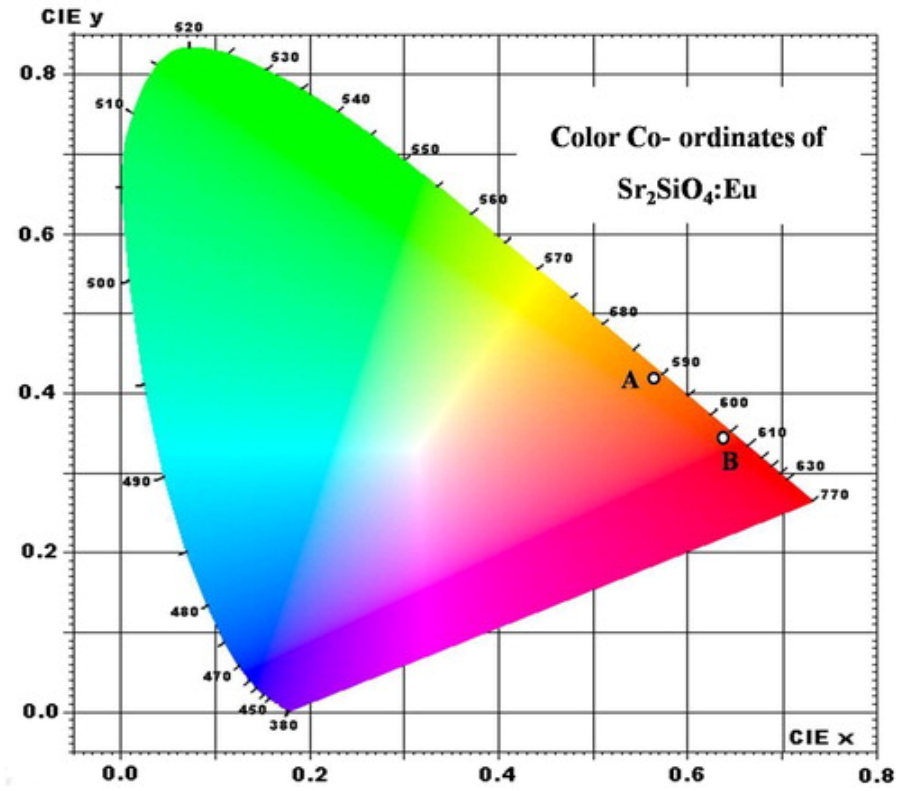

Display full size

4. Conclusions

The Eu^{3+} doped Sr_2SiO_4 are prepared by the novel solution combustion synthesis. FE-SEM confirms the formation of the nano-fiber nature of material. The bonding nature of the prepared host Sr_2SiO_4 and Eu^{3+} doped Sr_2SiO_4 well match with recent data of the published work. The PL emission spectra of the prepared Eu^{3+} doped Sr_2SiO_4 denote two characteristic different emissions at the 590 nm and 615 nm under 393 nm and 406 nm excitations respectively. These emissions observed at two different colors orange and red and therefore this phosphor may be applicable in solid state lighting for orange and red emission

In this article

5. References

1. A. J. Kenyon et al., Luminescence from erbium-doped silicon nanocrystals in silica: Excitation mechanisms, *J. Appl. Phys.* **91** (1), 367 (2002). DOI: 10.1063/1.1419210.
   Web of Science ® | Google Scholar

2. R. Schmechel et al., Luminescence properties of nanocrystalline Y2O3:Eu3+ in different host materials, *J. Appl. Phys.* **89** (3), 1679 (2001). DOI: 10.1063/1.1333033.
   Web of Science ® | Google Scholar

3. G. Wakefield et al., Luminescence properties of nanocrystalline Y2O3:Eu, *Adv. Mater.* **13** (20), 1557 (2001). DOI: 10.1002/1521-4095(200110)13:20<1557::AID-ADMA1557>3.0.CO;2-W.
   Web of Science ® | Google Scholar

4. F. M. Emen, N. Külcü, and A. N. Yazıcı, Synthesis, characterization and luminescence properties of the long afterglow phosphor Ba4Al14O25:Eu,Dy, *Eur. J. Chem.* **1** (1), 28 (2010). DOI: 10.5155/eurjchem.1.1.28-32.8.
   Google Scholar

5. S. H. M. Poort, W. Janssen, and G. Blasse, Optical properties of Eu2+activated orthosilicates and orthophosphates, *J. Alloy. Compd.* **260** (1–2), 93 (1997). DOI: 10.1016/S0925-8388(97)00140-0.
   Web of Science ® | Google Scholar

6. T. L. Barry, Fluorescence of Eu2+ activated phases in binary alkaline earth orthosilicate systems, *J. Electrochem. Soc.* **115** (11), 1181 (1968). DOI: 10.1149/1.2410935.
   Web of Science ® | Google Scholar

7. K. C. Mishra et al., First-principles investigation of the luminescence mechanism of Eu2+ in

10.1149/2.014203jss.

Web of Science ® | Google Scholar

8. H. C. Streit et al., Red, Green, and Blue Photoluminescence of Ba2SiO4:M (M = Eu3+, Eu2+, Sr2+), Nanophosphors. *Mater.* **6** (8), 3079 (2013). DOI: 10.3390/ma6083079.

Google Scholar

9. V. Singh et al., Characterization, luminescence and EPR investigations of Eu2+ activated strontium aluminate phosphor, *J. Noncrystal. Solids* **355** (50–51), 2491 (2009). DOI: 10.1016/j.jnoncrysol.2009.08.027.

Web of Science ® | Google Scholar

10. S. H. M. Poort, W. P. Blokpoel, and G. Blasse, Luminescence of Eu2+ in barium and strontium aluminate and gallate, *Chem. Mater. Mater.* **7** (8), 1547 (1995). DOI: 10.1021/cm00056a022.

Web of Science ® | Google Scholar

11. D. Wei et al., A new green-emitting barium zinc silicate: Eu2+ doped Ba2Zn3Si3O11, *Mater. Lett.* **99**, 122 (2013). DOI: 10.1016/j.matlet.2013.02.083.

Web of Science ® | Google Scholar

12. F. Clabau et al., Fluorescence and phosphorescence properties of the low temperature forms of the MAl2Si2O8:Eu2+ (M = Ca, Sr, Ba) compounds, *J. Solid State Chem.* **181** (6), 1456 (2008). DOI: 10.1016/j.jssc.2008.03.011.

Web of Science ® | Google Scholar

13. W. B. Dai et al., Structure and photoluminescence characteristics of europium(III) doped in CaAl2Si2O8 phosphors, *RSC Adv.* **4** (49), 25470 (2014). DOI: 10.1039/C4RA02213K.

Web of Science ® | Google Scholar

14. S. Janákova et al., Preparation and structural investigations of sol–gel derived Eu3+doped CaAl2O4, *J. Phys. Chem. Solids* **68**, 1147 (2007). DOI: 10.1016/j.jpcs.2006.12.034.

In this article

15. Y. Hu et al., Preparation mechanism and luminescence of Sr2SiO4:Eu phosphor from (Sr,Eu)CO3@SiO2 core-shell precursor, *Open J. Inorg. Chem.* **2** (1), 6 (2012). DOI: 10.4236/ojic.2012.21002.

Google Scholar

16. H. Nguyen, I. Yeo, and S. Mho, Identification of the two luminescence sites of Sr2SiO4:Eu2+ and (Sr,Ba)2SiO4:Eu2+ phosphors, *ECS Transactions* **28** (3), 167 (2010).

Google Scholar

17. J. Yang et al., Luminescence behavior of Eu3+ in CaSiO3:Eu3+(Bi3+) and Sr2SiO4:Eu3+(Bi3+), *J. Alloys Compds.* **454** (1–2), 506 (2008). DOI: 10.1016/j.jallcom.2007.02.079.

Web of Science ® Google Scholar

18. Q. Yanmin et al., Photoluminescent properties of Sr2SiO4:Eu3+ and Sr2SiO4:Eu2+ phosphors prepared by solid state reaction method, *J. Rare Earths* **27** (2), 323 (2009).

Web of Science ® Google Scholar

19. Y. Luo et al., Synthesis and luminescence properties of blue-emitting phosphor K2Ca2Si2O7:Ce3+, *Opt. Mater.* **36** (3), 723 (2014). DOI: 10.1016/j.optmat.2013.11.010.

Web of Science ® Google Scholar

20. B. S. Prathibha et al., Photo and thermo luminescence studies of Sr2SiO4:Eu3+ phosphor, *Int. J. Innov. Eng. Tech.* **6** (2), 190 (2015).

Google Scholar

21. I. P. Sahu, Orange-red emitting europium doped strontium ortho-silicate phosphor prepared by a solid state reaction method, *Luminescence* **1**, 11 (2016). DOI: 10.1002/bio.3188.

Google Scholar

22. B. S. Prathibha et al., Thermoluminescence studies on Sr2SiO4 nano powder, *Procedia Mater. Sci.* **5**, 944 (2014).

Google Scholar

In this article

23. C. Lu, and P. Wu, Reaction mechanism and kinetic analysis of the formation of Sr2SiO4 via solid-state reaction, *J. Alloys Compds.* **466** (1–2), 457 (2008). DOI: 10.1016/j.jallcom.2007.11.066.

Web of Science ® | Google Scholar

24. M. Catti et al., The β = α' phase transition of Sr2SiO4 I order-disorder in the structure of the α' Form at 383 K, *Acta Crystallogr. B Struct. Sci. Cryst.* **B39**, 674 (1983). DOI: 10.1107/S0108768183003213.

Google Scholar

25. J. Kaur, Y. Parganiha, and V. Dubey, Luminescence studies of Eu3+ doped calcium bromofluoride phosphor, *Phys. Res. Intern.* **494807**, 5 (2013). DOI: 10.1155/2013/494807.

Google Scholar

26. S. K. Gupta et al., Structure and site selective luminescence of sol–gel derived Eu:Sr2SiO4, *J. Luminescence* **132** (6), 1329 (2012). DOI: 10.1016/j.jlumin.2012.01.011.

Web of Science ® | Google Scholar

27. H. Liu et al., Luminescent properties of R+ doped Sr2SiO4:Eu3+ (R+= Li+, Na+ and K+) red-emitting phosphors for white LEDs, *J. Luminescence* **131** (11), 2422 (2011). DOI: 10.1016/j.jlumin.2011.05.042.

Web of Science ® | Google Scholar

28. Color Calculator Version 2, A Software from Radiant Imaging, Inc. (2007).

Google Scholar